ACS Energy Letters
http://pubs.acs.org/journal/aelccp

Thermally Regenerative Electrochemical Cycle for Low-Grade Heat Harvesting

Caitian Gao,[†] Seok Woo Lee,*[,†] and Yuan Yang*[,‡]

[†]School of Electrical and Electronic Engineering, Nanyang Technological University, Singapore
[‡]Department of Applied Physics and Applied Mathematics, Columbia University, New York, New York, United States

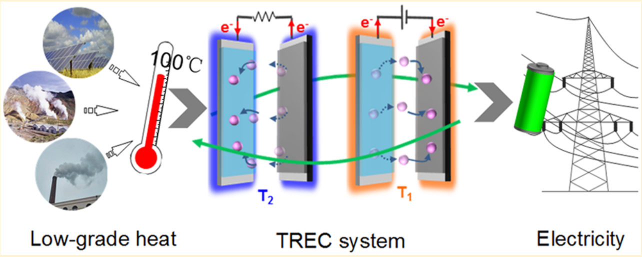

ABSTRACT: Tremendous low-grade heat (i.e., <130 °C) exists in solar thermal, geothermal, and industrial waste heat. Efficient conversion of low-grade heat to electricity can recover these wasted resources and reduce energy consumption and carbon footprint. Along with thermoelectrics and thermogalvanic cells, thermally regenerative electrochemical cycle (TREC) has attracted wide attention recently, because it has a high temperature coefficient (>1 mV/K), high efficiency, and low cost. In TREC, conversion to electricity is realized by charging−discharging an electrochemical cell at different temperatures. In this Perspective, we will discuss the principle of TREC and recent progress, such as new material systems and mechanisms. More importantly, we will give our opinions on the challenges and future directions of this field, including fundamental understanding, material design, and system engineering.

A tremendous amount of low-grade heat (e.g., < 130 °C) exists around us in various forms, such as solar/geothermal heat[1,2] and waste heat[3] produced by vehicles and industries (Figure 1a).[4] A large portion of primary energy produced in the world is rejected as low-grade waste heat because of the inefficiencies during the energy conversion; for example, in the U.S., the portion rejected as low-grade heat reached 66.4% in 2016.[5] Therefore, the conversion and reuse of low-grade heat is one of the most promising ways to solve worldwide energy challenges. However, the conversion of low-grade thermal energy to other types of energy, such as electricity, remains highly challenging as a result of the distributed nature of heat sources and the low temperature differential with the environment.

Among the various approaches for harvesting heat, thermoelectrics has been one of the most promising and widely investigated. Thermoelectric devices are based on the voltage generated across a conductive material under a temperature gradient, the so-called Seebeck effect. The effect is described using the Seebeck coefficient, defined as the ratio of voltage difference and temperature difference ($S = \mathrm{d}V/\mathrm{d}T$). The efficiency of a thermoelectric device is determined by the figure of merit $\mathrm{ZT} = \frac{S^2 \sigma T}{k}$ where σ and k are the electrical and the thermal conductivities, respectively.[6,7] For practical low-temperature thermoelectric applications, a ZT of 3−4 is desirable.[6,8] However, despite remarkable progress in recent years, ZT remains below 1.5 at temperatures <150 °C. One major reason for this is that S is only about 0.2 mV/K for state-of-the-art materials.

A phenomenon that is apparently similar to the Seebeck effect exists in electrochemical systems, arising from the temperature dependence of electrode potential in electrochemical reactions. For an electrochemical reaction ($\mathrm{A} + ne^- \rightarrow \mathrm{B}$), the temperature coefficient (α) of its electrode potential is $\alpha = \frac{\mathrm{d}V}{\mathrm{d}T} = \frac{S_\mathrm{B} - S_\mathrm{A}}{nF}$, where S_A and S_B are the partial molar entropies of A and B, respectively, and F is the Faraday constant.[9] For some systems, α can be as high as 1−3 mV/K, one order of magnitude higher than S of thermoelectric materials, making them attractive for heat harvesting.[10−12] There are two major approaches to utilize such temperature coefficients. The first is to employ a thermogalvanic cell in the same configuration as a thermoelectric device.[13,14] However, in a thermogalvanic cell, as ion transport occurs simultaneously with thermal conduction, the efficiency is limited by the low ionic conductivity of the electrolyte. As a result, the typical efficiency is limited to an equivalent ZT of <0.1 (e.g., efficiency is 0.7% of Carnot efficiency (η_c) at ΔT = 5K).[12,15,16]

The second approach is to create a thermodynamic cycle, termed thermally regenerative electrochemical cycle (TREC).[17] In TREC, an electrochemical cell is constructed to have two different electrodes, with a temperature coefficient (α_cell) that is the difference between the temperature coefficient of the positive electrode (α_+) and that of the negative electrode (α_-). $\alpha_\mathrm{cell} = \Delta S_\mathrm{cell}/nF$, where ΔS_cell is the total entropy change in the full cell reaction. If $\alpha_\mathrm{cell} > 0$, the cell is first heated to a high temperature (T_H), and discharged at T_H. Subsequently, the cell is cooled to a low temperature (T_L) at open circuit, where the open-circuit voltage becomes smaller because of a positive α_cell; then the cell is

Received: June 30, 2017
Accepted: August 31, 2017
Published: August 31, 2017

ACS Publications

DOI: 10.1021/acsenergylett.7b00568
ACS Energy Lett. 2017, 2, 2326−2334

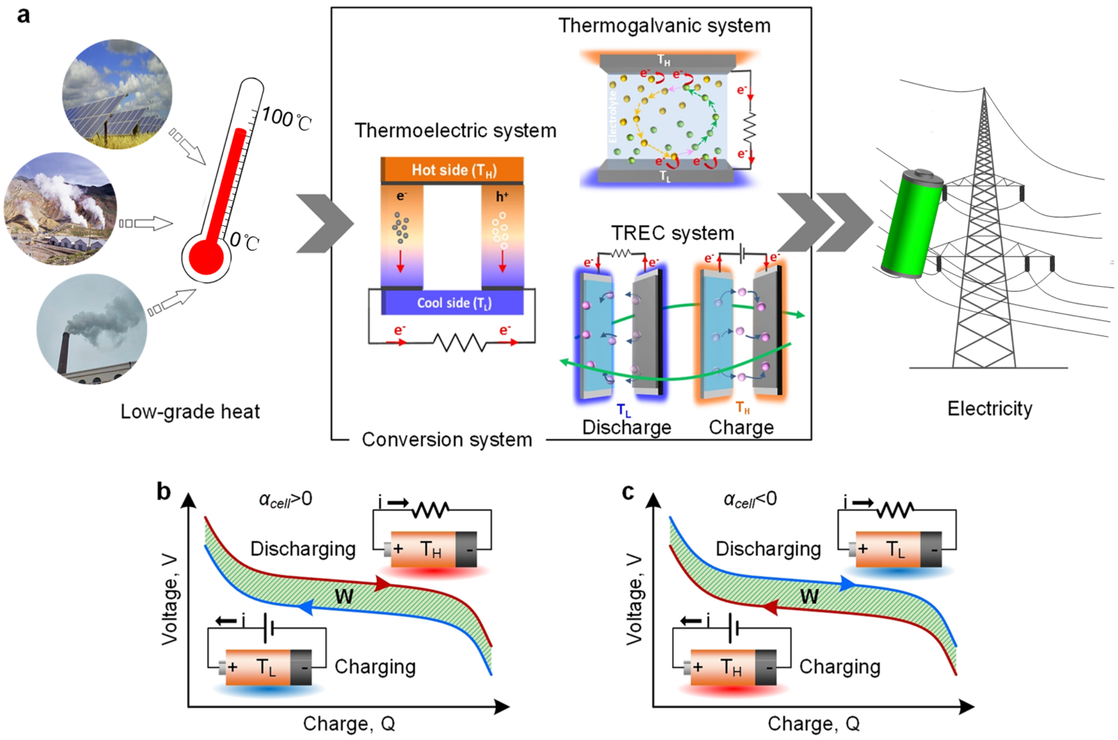

Figure 1. (a) Schematic of a system to harvest low-grade heat sources, with three conversion systems [thermoelectric, thermogalvanic, and thermally regenerative electrochemical cycle (TREC)] shown. (b) Schematic of thermodynamic cycle with $\alpha_{cell} > 0$. (c) Schematic of thermodynamic cycle with $\alpha_{cell} < 0$. Photographs in panel a are adapted with permission from ref 1 (copyright 2014 Elsevier), ref 2 (copyright 2005 Elsevier), and ref 3 (copyright 2016 Elsevier).

recharged at T_L to the initial state of charge (SOC) to complete a cycle (Figure 1b). If $\alpha_{cell} < 0$, the cell is first cooled to T_L and discharged; it is then heated to T_H and recharged to initial SOC (Figure 1c). Both thermodynamic cycles shift the charging curve lower than the discharging curve as compared to the typical charging and discharging process; therefore, net work is produced during these cycles because of the voltage differences. Decades ago, TREC received significant attention, but the focus was mostly on high-temperature thermal energy (>500 °C).[17] Recently, multiple TREC systems for harvesting low-grade heat have been reported.[8−22] For example, Lee et al. have demonstrated a TREC system with a 3.7% efficiency (25% of η_c) when only active materials are considered. In this Perspective, we focus on TREC for harvesting low-grade heat. Starting with a discussion of the working principle and theory of TREC, we then review recent progress in the field and present our thoughts on the challenges that lie ahead and future directions for research.

> Both thermodynamic cycles shift the charging curve lower than the discharging curve as compared to the typical charging and discharging process; therefore, net work is produced during these cycles because of the voltage differences.

Working Principle and Theory. As defined, TREC is a thermodynamic cycle, where heat is absorbed at T_H and partially rejected at T_L. The difference is converted to electrical work. This can be clearly seen in the temperature−entropy plot (Figure 2a). The efficiency (η) of TREC can be calculated as the net work (W) divided by the thermal energy input. If the enthalpy change ΔH and the entropy change ΔS are assumed to be the same at T_H and T_L, which is a good approximation when $\Delta T = (T_H - T_L)$ is not large, the maximum W is $\Delta T \Delta S$. The energy input to complete the cycle includes two parts: heat absorbed at T_H ($Q_H = T_H \Delta S$) and external heat required to raise the temperature of the system (Q_{HR}). As part of heat rejected from the cooling process can be reused for the heating process through heat recuperation, Q_{HR} can be expressed as $Q_{HR} = (1 - \eta_{HR})C_p\Delta T$, where C_p is the total heat capacity of the electrochemical cell and η_{HR} is the efficiency of the heat recuperation, defined as the ratio of heat transfer from the cooling process to the heating process to energy needed for heating the cell from T_L to T_H. Consequently, η can be expressed as[20]

$$\eta = \frac{W}{Q_H + Q_{HR}} = \frac{\Delta T \Delta S - E_{loss}}{T_H \Delta S + (1 - \eta_{HR})C_p \Delta T} \tag{1}$$

where E_{loss} is the energy loss due to the cell electrical resistance ($I(R_H + R_L)$). I is the current used in discharging and charging. R_H and R_L are the internal resistance at T_H and T_L, respectively. Note that $\Delta T \Delta S = \alpha_{cell}\, Q_c\, \Delta T$, where Q_c is the charge capacity of the cell and α_{cell} is the temperature coefficient of the electrochemical cell. The efficiency then becomes

$$\eta = \eta_c \frac{1 - I(R_H + R_L)/|\alpha_{cell}|\Delta T}{1 + \eta_c(1 - \eta_{HR})/|Y|} \tag{2}$$

where $Y = \alpha_{cell}\, Q_c/C_p$. From eq 2, we can see that when internal resistance is neglected, the efficiency η depends on $Y = \alpha_{cell}\, Q_c/C_p$. Similarly, for a given electrode material, the figure of merit y is defined as $\alpha q_c/c_p$, where q_c is the specific charge capacity and c_p

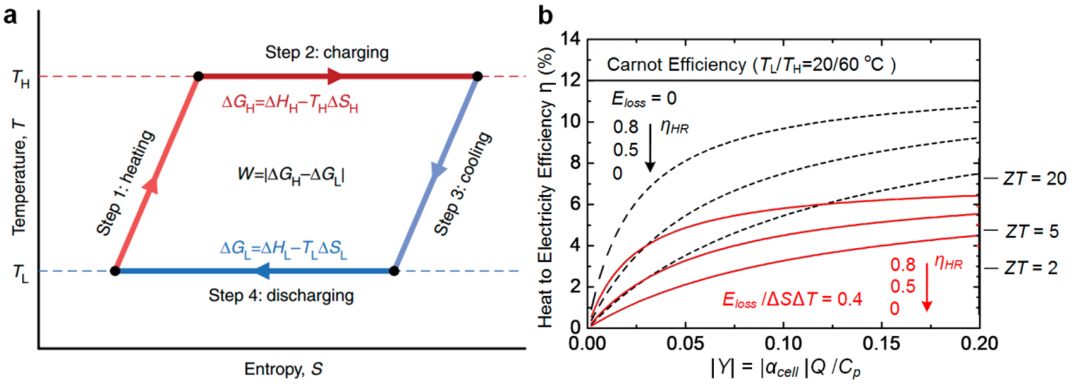

Figure 2. (a) Temperature–entropy (T–S) diagram of a thermally regenerative electrochemical cycle (TREC) between T_L and T_H. (b) Thermal to electricity efficiency of TREC when T_L/T_H is 20/60 °C. Black dotted lines correspond to zero energy losses (E_{loss}) from cell resistance. Red lines correspond to a E_{loss} = 40% of the theoretical energy gain ($\Delta T \Delta S$). For each color, the graphs correspond to heat recuperation efficiencies η_{HR} of 0.8, 0.5, and 0 from top to bottom. The ZT values on the right-hand axis are theoretical values required by thermoelectric devices (working between 20 and 60 °C) to reach corresponding efficiencies. Panel a is adapted with permission from ref 20. Copyright 2014 Nature Publishing Group.

is the specific heat of an electrode. Hence, y is a dimensionless parameter to describe the material requirements for high efficiency. Consequently, it is clear that a higher temperature coefficient (α), a higher specific charge capacity (q_c), and a smaller specific heat (c_p) of materials lead to higher efficiency for heat-to-electricity conversion.[20] In addition, low-voltage polarization and effective heat recuperation can also improve the efficiency. The expression for y appears to be similar to the figure of merit, z, in thermoelectric materials, but it should be noted that α, q_c, and c_p are not coupled together; therefore, it is possible to tune them separately to maximize η. A thorough derivation of the efficiency can be found in the literature.[20]

The expression for y appears to be similar to the figure of merit, z, in thermoelectric materials, but it should be noted that α, q_c, and c_p are not coupled together; therefore, it is possible to tune them separately to maximize η.

To provide a better comparison between TREC and other techniques, the efficiency η versus Y is plotted in Figure 2b for T_L/T_H of 20/60 °C, which indicates a Carnot efficiency (η_c) of 12.0%. If $Y = 0.1$ [e.g., α_{cell} = 2 mV/K, specific capacity (q_c) of 75 mAh/g, and specific heat (c_p) of 2.7 J/g K for each electrode], and η_{HR} = 50%, η can reach 4.5% and 7.5% for $E_{loss}/\Delta T \Delta S$ of 0.4 and 0, respectively. Such results illustrate the potential of TREC for low-grade heat harvesting.

Besides conversion efficiency, power density is also an important parameter for energy conversion. For TREC systems, maximum power output is $P_{max} = \frac{(\alpha_{cell}\Delta T)^2}{8(R_H + R_L)}$, when $I = \frac{\alpha_{cell}\Delta T}{2(R_H + R_L)}$,[17] and the specific power is typically in the order of 1–10 W/kg, which is about 1–2 orders of magnitude less than that of thermoelectric devices. The major reason for the low power density is high cell resistance, which originates from the much slower transport of ions than of electrons. One important focus of recent studies has been how to improve battery kinetics to enhance power density.[23,24]

Recent Progress on TREC. The concept of TREC dates back to 1886, when Case first reported a system based on Sn|Sn(II), Cr(III), Cr(II)|carbon with T_L/T_H of 10/90 °C.[25] After that, the major interest was to harvest high-temperature heat (>500 °C) for aerospace and nuclear applications by 1970s using designs like molten metal/halide cells. A good summary of work prior to 1980 can be found in a report by NREL.[17] However, harvesting low-grade heat by TREC had not been well studied because of

Table 1. Comparison of the TREC Systems

system (positive electrode, negative electrode)	α_+ (mV/K)	α_- (mV/K)	α_{cell} (mV/K)	ion-selective membrane	electrical assistance	efficiency (%)	ref
$Fe(CN)_6^{3-/4-}$, $Cu(NH_3)_4^{2+}/Cu(NH_3)_2^{+}$	−1.6 ± 0.025	1.39[a]	−2.9	yes	no	8.30–12.40 (30–90 °C with 100% η_{HR})	18, 26
CuHCF, Cu/Cu^{2+}	−0.36	0.83	−1.20	yes	yes	3.70 (10–60 °C with 0% η_{HR}) 5.70 (10–60 °C with 50% η_{HR})	20, 26
$Fe(CN)_6^{3-/4-}$, FeHCF	1.46 ± 0.02	0.00 ± 0.03	−1.45 ± 0.03	yes	no	2.00 (20–60 °C with 70% η_{HR})	21, 26
Cu^{2+}/Cu, $Cu/Cu(NH_3)_4^{2+}$	−0.3	−1.0	_	yes	no	0.86 (25–70.6 °C with 0% η_{HR})	19, 27
NiHCF, Ag/AgCl	−0.62	0.12	−0.74	no	yes	3.50 (15–55 °C with 70% η_{HR})	28
activated carbon on both electrodes	_	_	0.6	no	yes	5.00 (0–65 °C theoretical value)	22

[a] This value was calculated according to the entropy change listed in ref 18.

the limited efficiencies, which arise from the voltage gain ($|\alpha_{\text{cell}}\Delta T|$) being similar to resistive losses ($I(R_H + R_L)$). In recent years, various redox pairs with fast kinetics have been reported and have led to novel material systems which can enhance TREC efficiency for low-grade heat harvesting. In this section, we review representative examples, summarized in Table 1, to illustrate their underlying concepts and performance.

$Fe(CN)_6^{3-/4-}$, $Cu(NH_3)_4^{2+}/Cu(NH_3)_2^{+}$ System. Hammond et al. demonstrated a TREC system to convert low-grade heat directly from solar energy to electrical energy in 1979.[18] As shown in Figure 3, two cells, one at T_H (hot state) and the other at T_L (cold state), are connected by pumps which recycle the reaction products. In each cell, two half-reactions are separated by membranes which allow only the passage of charge carriers of M^+ and X^-. The cycle is realized by continuous electrochemical reaction of A and B to produce C and D in the hot cell and the reaction of C and D to produce A and B in the cold cell. The voltage difference in the two cells due to temperature effect provides power to the external load (R_L). In such a design, reaction products in one cell flow to the other by pump, leading to continuous operation and regeneration of reactants. The two redox pairs $Cu(NH_3)_4^{2+}/Cu(NH_3)_2^{+}$ (corresponding to A/C) and $Fe(CN)_6^{4-/3-}$ (corresponding to B/D) result in a high α_{cell} of −2.9 mV/K, which is among the highest values reported to date. The specific reaction in the hot cell and cold cell (reverse reaction) is given by

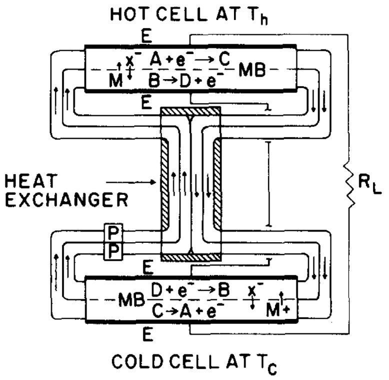

Figure 3. Schematic of the $Fe(CN)_6^{3-/4-}$, $Cu(NH_3)_4^{2+}$/ $Cu(NH_3)_2^{+}$ system. In this figure, the redox pairs are represented by A/C and B/D in general. The electrodes are marked by E, semipermeable ion transport membranes by MB, pumps by P, external load as L, and the current-carrying ions as M^+ and X^-. Reproduced with permission from ref 18. Copyright 1979 Elsevier.

$$Cu(NH_3)_4^{2+} + Fe(CN)_6^{4-} \leftrightarrow Cu(NH_3)_2^{+} + Fe(CN)_6^{3-} + 2NH_3$$

The design was reported to achieve an η equivalent to 50−75% of η_c between 30 and 90 °C, with an assumption of 100% heat recuperation. However, it is restricted by a large internal resistance and suffers from poor stability due to the precipitation of $Cu_2Fe(CN)_6$ several hours into its operation.

Prussian Blue Analog-Based Systems. Soluble redox pairs have fast kinetics to reduce cell resistance for TREC; however, the typically low solubility of redox ions (e.g., 0.4 M for $Fe(CN)_6^{3-/4-}$) indicates low q_c and high c_p. Thus, significant energy is needed to heat the electrolyte. As practical heat recuperation can reach only 80−90% for fluidic systems, this remarkably reduces the overall conversion efficiency. To address this issue, a team led by Yi Cui and Gang Chen demonstrated several TREC systems based on solid Prussian blue analog (PBA) materials with high specific capacity, low specific heat, and fast kinetics. In PBAs, transition-metal ions are linked by cyano groups to form a rock salt-type network, and alkaline ions sit in the center of each cube. Prussian blue analog has an open structure, resulting in an extremely fast kinetics and good stability upon ion insertion and removal. Therefore, a long cycle life >10 000 times is attained.[29]

The first demonstrated PBA-based TREC consists of copper hexacynoferrate (CuHCF) cathode and Cu/Cu^{2+} anode in an aqueous electrolyte. The system has a high α_{cell} of up to −1.2 mV/K (Table 1). When the cell is charged at T_H (60 °C) and then discharged at lower temperature T_L (10 °C) at a higher voltage (Figure 4a,b), the electrical energy produced is 5.2 J/g. The thermal to electricity conversion efficiency reaches 3.7%, which is equivalent to 25% of η_c, even without heat recuperation. At η_{HR} conservatively assumed at 50%, the conversion efficiency can be significantly increased to 5.7%.

The demonstrated TREC system requires external electricity to charge the battery back to its initial state. To resolve this shortcoming, the authors of the study designed a charging-free electrochemical cell as depicted in Figure 4c.[21] The overall energy-harvesting cycle is the same as that in the previous case. However, at the neutral state, both electrodes have same electrochemical potential, and the signs of the temperature coefficient of the electrodes are opposite. Therefore, the change of temperature from T_1 to T_2 switches the polarity of the cell and the cell can be discharged at both temperatures without applying an external voltage. The key aspect of the improved system is the choice of the electrode materials such that voltage change due to temperature variation is larger than cell voltage. The full cell voltage change versus time during the thermodynamic cycle is shown in Figure 4d. The corresponding η is 0.68% without any heat recuperation and 2.0% with η_{HR} of 0.7.

The systems mentioned above all need to use certain ion exchange membranes to avoid the mixing of cathode and anode. However, such membranes not only increase the overall cost of the system but also reduce the system efficiency and long-term cycling, as it is difficult to completely block the penetration of the ions after prolonged operation. Membraneless systems can be used, with the restriction that that any chemical species soluble in the electrolyte should not induce adverse side-reactions other than the desired half-cell reactions. In a recent report, such a system is demonstrated with nickel hexacynoferrate (NiHCF) cathode, Ag/AgCl anode,[28] in which no adverse side reaction is introduced as shown below:

$$\text{Cathode:} \quad KNiFe(CN)_6 + K^+ + e^- \rightarrow K_2NiFe(CN)_6$$

$$\text{Anode:} \quad Ag + Cl^- \rightarrow AgCl + e^-$$

During long-term operation, the system shows a low capacity fading rate and high Columbic efficiency at different current rates. The corresponding thermal-to-electricity efficiency (η) reaches 2.9% (24% of η_c) after 50 cycles at C/2 and η_{HR} of 0.7.

$Cu\text{-}NH_3/Cu(NH_3)_4^{2+}$ System. The Logan group has also demonstrated a TREC system using an ammonia-based battery.[19] In this system, they applied Cu^{2+}/Cu as a cathode and $Cu\text{-}NH_3/Cu(NH_3)_4^{2+}$ as an anode. The schematic of the cell is shown in Figure 5a. The electricity is produced by the formation of metal ammine complexes, and the electrochemical reactions are as follows:

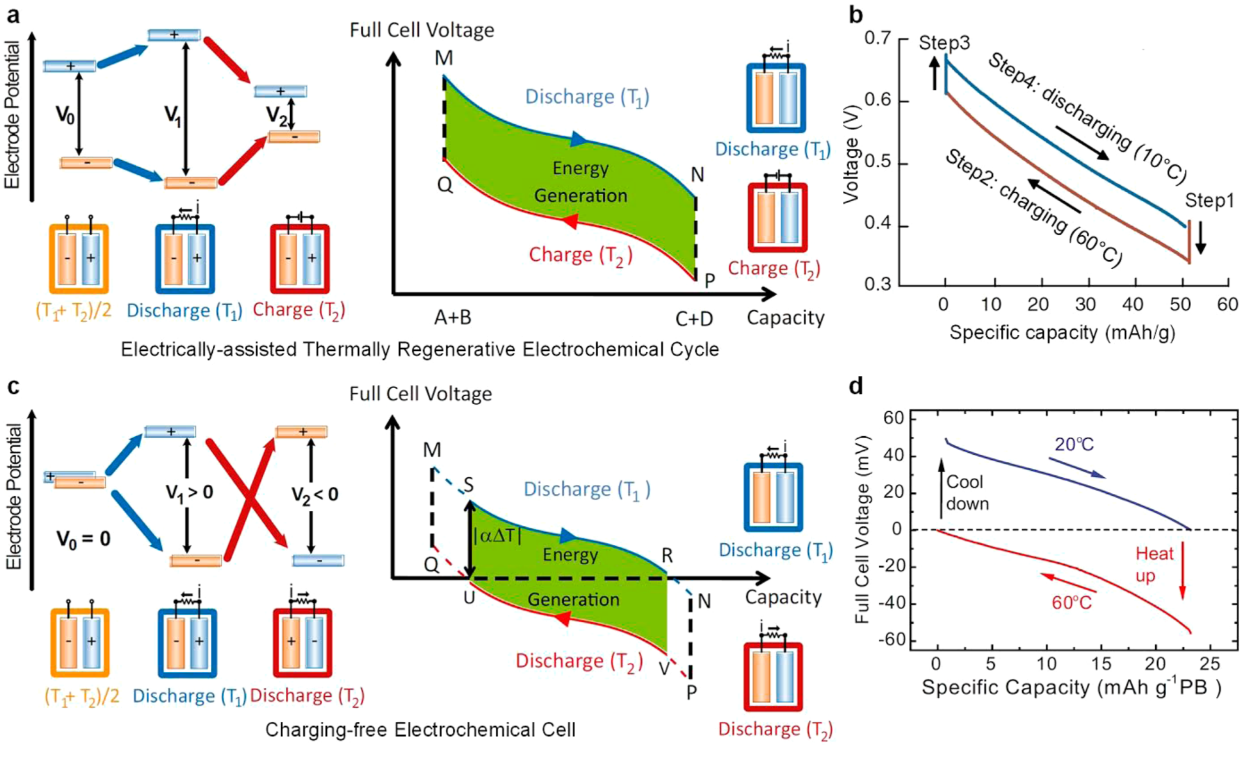

Figure 4. Schematics and performances of TREC cells with (a, b) and without (c, d) electrical assistance. (a) Electrode potential changes in positive and negative electrodes and the full cell in an electrically assisted thermal cycle. (b) A voltage plot of the cell versus the specific capacity of CuHCF for one thermodynamic cycle. (c) Electrode potential changes in positive and negative electrodes and the full cell in a charging-free thermal cycle. (d) Cycling operation of the charging-free system. The cell is operated between 20 and 60 °C. Panels a, c, and d are adapted with permission from ref 21. Copyright 2014 National Academy of Sciences. Panel b is adapted with permission from ref 20. Copyright 2014 Nature Publishing Group.

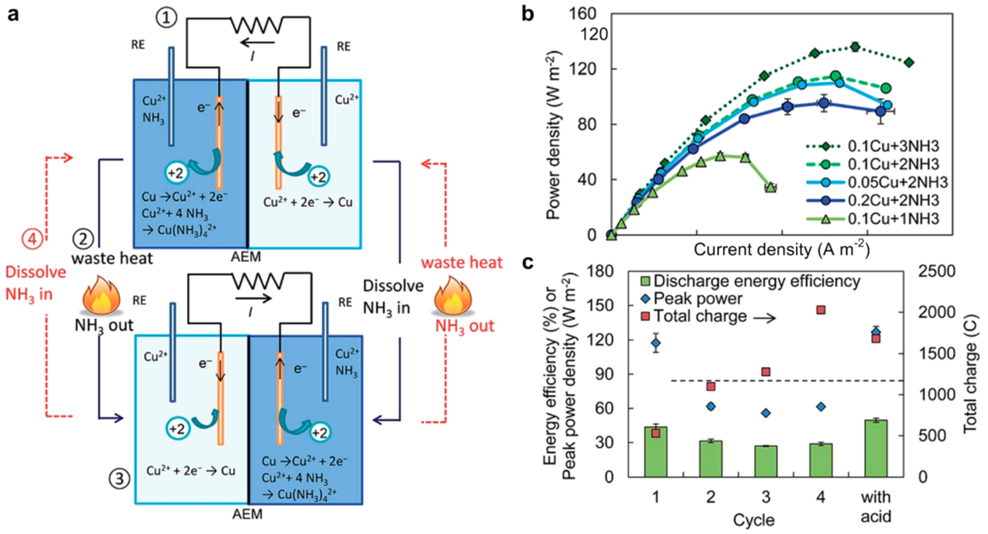

Figure 5. (a) Schematic of the ammonia-based electrochemical cell for low-grade heat harvesting. Four processes are operated in this system. (b) Change in power density with various Cu (II) and ammonia concentration. (c) Change in energy efficiency, power density, and total charge in the ammonia-based cell over successive cycles. Reproduced with permission from ref 19. Copyright 2015 Royal Society of Chemistry.

Cathode: $Cu^{2+}(aq) + 2e^{-} \rightarrow Cu(s)$

Anode: $Cu(s) + 4NH_3(aq) \rightarrow Cu(NH_3)_4{}^{2+} + 2e^{-}$

In this system, the waste heat is used to regenerate the electrolyte; therefore, the reactants are chemically regenerated by thermal energy, and the thermodynamic cycle is completed. As shown in Figure 5b, the power heavily depends on the electrolyte concentration, because the potential difference is governed by the Nernst equation for NH_3. Increasing the anodic NH_3 concentration from 1 to 3 M improved the power production from 57 ± 2 $W \cdot m^{-2}$ to the maximum value of 136 ± 3 $W \cdot m^{-2}$. However, the byproduct, $Cu(OH)_2$, reduced the energy efficiency after four cycles (Figure 5c). As a result, acid had to be added to the catholyte to dissolve $Cu(OH)_2$ and regenerate the system. However, this remedy may not be suitable for

DOI: 10.1021/acsenergylett.7b00568
ACS Energy Lett. 2017, 2, 2326−2334

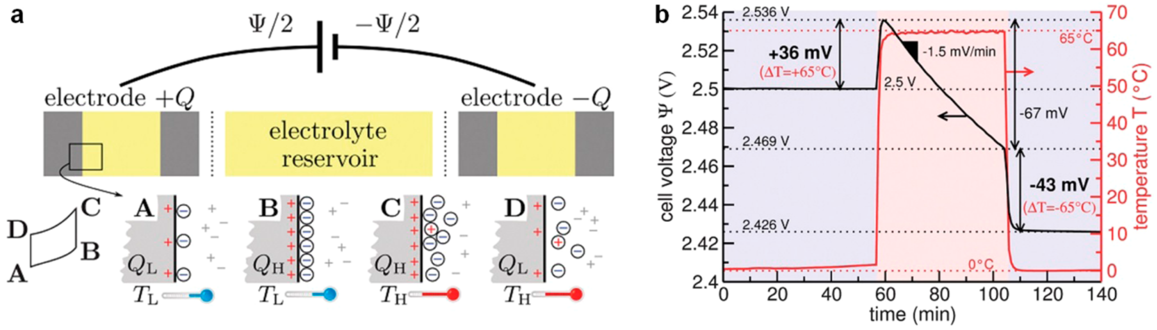

Figure 6. (a) Model of supercapacitor with two parallel plates in the electrolyte reservoir. (b) Variation of the open-circuit potential when cycling the fully charged cell between 0 and 65 °C. Reproduced with permission from ref 22. Copyright 2015 Royal Society of Chemistry.

practical operations, making the system difficult to adapt for long-term thermal energy harvesting.

Electrical Double-Layer-Based Cycle. Besides using entropy change due to redox reaction, the entropy change in electrical double-layer capacitors can also be utilized to construct a similar cycle for harvesting thermal energy, as shown in Figure 6. Recently, Härtel et al. reported a voltage change from 2.50 to 2.536 V when temperature changes from 0 to 65 °C, corresponding to α_{cell} of 0.6 mV/K (Figure 6b).[22] Such α_{cell} is attributed to the change of double-layer capacitance affected by the ionic entropy during the thermodynamic cycle. Efficiencies as high as 5% are theoretically predicted and experimentally demonstrated. However, the cell voltage has a linear decay in the hot cell with a rate of −1.5 mV/min. Thus, the system needs to be operated within a certain time scale and requires a rapid charging and discharging process.

Challenges and Future Direction. Recent years have witnessed plenty of progress in TRECs for harvesting low-grade heat; however, significant improvements are still needed for use of TRECs to be practical. This requires both fundamental understanding of design principles and material and system engineering. In this section, we discuss our thoughts on existing challenges and future directions in the field, with specific emphasis on the fundamental understanding of temperature coefficient α, materials design, and system engineering.

Fundamental Understanding of α. A critical step in developing high-performance TRECs is to determine a suitable redox pair with high α. A comprehensive list of α of common redox pairs in aqueous systems has been calculated using thermodynamic data by deBethune et al.[9] and Bratsch[30] based on thermodynamic data. Most experimental results are consistent with theoretical calculations, but discrepancy was also observed, indicating that more theoretical work is needed to understand α in electrochemical systems. Table 1 provides a list of α of key redox and new materials in TREC.

From material thermodynamics, the total entropy change in a chemical reaction can generally be expressed as follows: $\Delta S = \Delta S_{\text{ion}} + \Delta S_{\text{phonon}} + \Delta S_{\text{config}} + \Delta S_{\text{electron}} + \Delta S_{\text{other}}$, where the five terms correspond to entropy of ions in electrolyte, phonon entropy in the solid phase, configurational entropy, electron entropy, and other entropy, respectively. Entropy of ions in an electrolyte is fundamentally related and highly relevant to its solvation structure and concentration. Simulations of ion entropy have been carried out by various models, including molecular dynamics and continuity models, and show good consistency with experimental results.[31,32] Phonon entropy can be derived based on density functional theory calculations and measurements of phonon density of states; a comprehensive review of this topic can be found in the literature.[33] Configurational entropy is related to arrangement of ions in the solid phase. Electron entropy is typically small, but it may play an important role when phase transition is involved, such as in $LiFePO_4$.[34]

Although the entropy change in electrochemical reactions can generally be described as stated above, few studies have focused on its origins. For example, the Fultz group studied the temperature coefficient of a $Li/LiCoO_2$ cell and concluded that α arises from change in phonon density of states (DOS) and configuration entropy of Li ions.[35] However, it is not yet known how such change in phonon DOS is related to variations in material properties such as lattice parameters, bonding strength, and phase transition. It is also unclear why $LiCoO_2$ and $Li(Ni_xMn_yCo_z)O_2$ have drastically different α, although their material structures are almost identical.[36] Similarly, it is not understood why PBAs also show different α of 0.00 ± 0.03 mV/K (FeHCF), −0.36 mV/K (CuHCF), and −0.62 mV/K (NiHCF) in spite of their similar structure and reaction nature.[20,21,28] In the future, it is important to answer the following questions: How does entropy change correlate with material structures and properties? How can electrode structure and composition and electrolyte be designed or chosen to optimize entropy change? How can entropy change be better predicted by simulations? Detailed and quantitative understanding of these topics will advance our knowledge on the correlation between entropy change and material structures and properties and guide the development of high-performance electrochemical materials for efficient conversion of heat to electricity.

Materials Design. Besides fundamental understanding to develop materials with high α and figure of merit Y, material design is also critical to realize high-performance devices with high power and long cycle life. Practical TRECs may need a cycle life of >10 000 to be economically attractive. On the basis of phases of materials involved, there are two critical areas to focus on.

Besides fundamental understanding to develop materials with high α and figure of merit Y, material design is also critical to realize high-performance devices with high power and long cycle life.

(1) Advanced Membrane. In many TREC systems, a membrane is needed to separate two electrolytes for the two electrodes. Imperfections in such membranes could cause two

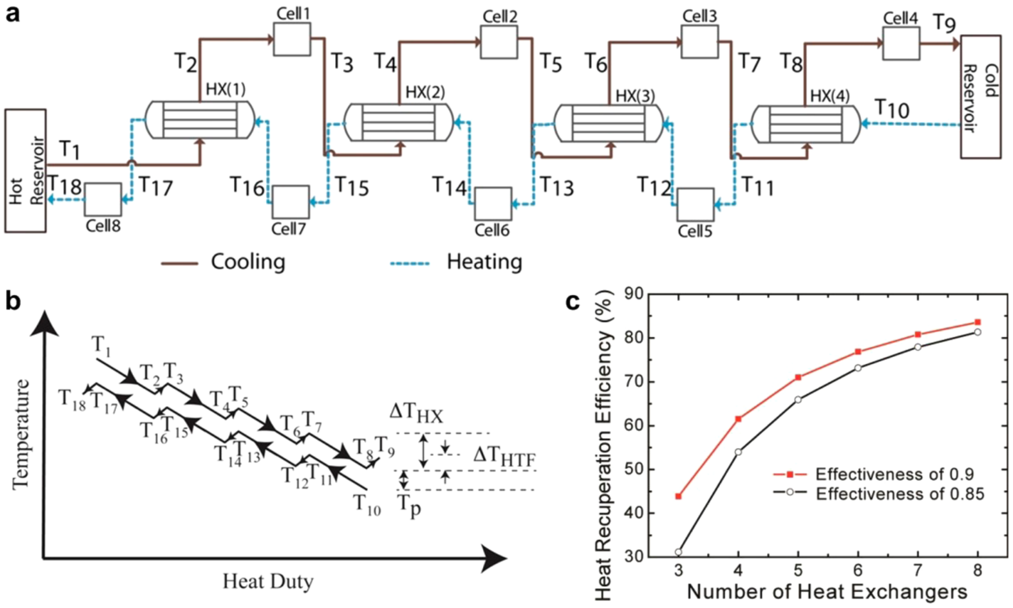

Figure 7. Heat recuperation design with heat exchangers. (a) A design for heat recuperation in TREC with heat exchangers. This design shows four heat recuperation steps, but it can be extended to any number of recuperation steps by adding more counter-flow HXs and cells. (b) Pinch diagram of the $n = 4$ step heat recuperation cycle in panel a at a given time. T_1 and T_{10} are the temperatures of hot and cold reservoirs, respectively. (c) Simulation results of the dependence of heat recuperation efficiency on the number of heat exchangers. The red and black lines represent heat exchange effectiveness of 0.9 and 0.85, respectively. Panels a−c are adapted with permission from ref 20. Copyright 2014 Nature Publishing Group.

problems, namely, diffusion of ions across the membrane and direct reaction between redox on two sides of the membrane. The first lowers the Coulombic and overall conversion efficiencies, while the second results in precipitation on the membrane and leads to higher resistance. For example, Hammond et al. reported that resistance increased after several hours because of the formation of $Cu_2Fe(CN)_6$ on the $BaSO_4$ precipitate membrane.[18] To solve these two challenges, advanced membranes that have low or zero permeability to reactants must be used. Such membranes can be made by coating[37,38] and even using ion-selective ceramic-based solid electrolytes.[39,40]

(2) Material Engineering of Solid Electrodes. Solid electrodes have the advantages of low specific heat and high charge capacity, which lead to a Y value that is higher than that of liquid electrolytes, but they typically have much slower kinetics than soluble redox pairs. Therefore, it is important to design materials to enable fast kinetics, with aspects such as open structure at the molecular level, nanostructuring, and surface coating offering scope for improvement. At the molecular level, for example, Prussian blue analog nanoparticles may be used, as they have open structures to facilitate ion diffusion into the solid electrode.[29] Nanostructures, on the other hand, could provide a larger surface area and shorter diffusion paths than micrometer-sized particles to enhance kinetics. Surface coating may also improve interfacial ionic transport to reduce cell resistance.[41] Besides fast kinetics, it is also important to design materials to realize long-term stability, especially at elevated temperatures.

System Design. Besides developing high-performance materials for TREC, it is also critical to design the system to efficiently transfer and manage heat. Specifically, it is important to effectively recuperate heat to save energy for heating cells. In TRECs, a significant amount of energy is needed to heat cells and can account for 60−70% of heat input in a cycle. Therefore, an efficient recuperation system to transfer the rejected thermal energy from the cooling phase to the heating phase can significantly enhance efficiency. In liquid redox configurations (e.g., Figure 3), the two electrolytes can directly act as heat-transfer fluids and help attain heat recuperation efficiencies as high as 80−90%. Solid cells are a more difficult problem to solve. A direct contact between a hot cell and a cold cell can result in an η_{HR} of at most 50%. However, through careful design, such as the use of multiple heat exchangers, the recuperation efficiency can in principle be boosted to 70−80% (Figure 7). Although efficient concepts have been demonstrated, how to design high-efficiency and low-cost heat recuperation systems for both liquid-based and solid-based TREC systems remains an open question. A detailed analysis of how heat recuperation efficiency affects overall conversion efficiency and power can be found in the literature.[42]

Summary and Outlook. TREC is an electrochemical cycle for heat harvesting, where an electrochemical cell is charged−discharged at different temperatures, so that the discharge is at a higher voltage and enables the heat absorbed during the cycle to be extracted as electricity. Recent progress in materials and systems for TRECs offer new possibilities for designing practical systems with long-term stability and low cost. Although significant progress has been made, there is still a lack of fundamental understanding of temperature coefficient in TREC, especially how it correlates with material structure and properties. Such understanding can guide us to design new materials with high temperature coefficient and figure of merit Y. At the same time, advanced materials and system designs are also needed to enhance power density, cycle life, stability at elevated temperature, and system efficiency of TRECs. We believe that there are still many questions to answer and plenty of opportunities to explore from atomic to system levels. Multidisciplinary studies across materials science, mechanical engineering, chemistry, chemical engineering, and computational science will lead to more advanced systems for efficient conversion of low-grade heat to electricity in the future.

■ AUTHOR INFORMATION

ORCID

Yuan Yang: 0000-0003-0264-2640

Notes

The authors declare no competing financial interest.

Biographies

Caitian Gao is a postdoctoral research fellow in Nanyang Technological University. Her research field is designing low-dimensional materials and constructing electrochemical/photoelectrochemical systems for energy harvesting and storage. She received her Ph.D. degree in physics from Lanzhou University in 2015. Currently she is focusing on harvesting thermal energy by electrochemical systems.

Seok Woo Lee is an assistant professor in the School of Electrical and Electronic Engineering, Nanyang Technological University. He received his B.S. in mechanical engineering from Pohang University of Science and Technology (POSTECH) in 2003 and his Ph.D. in mechanical engineering from Korea Advanced Institute of Science and Technology (KAIST) in 2008. Then, he worked as a postdoctoral scholar and a research associate at Stanford University for about 6 years. His research interests are in electrochemical systems for energy storage and conversion.

Yuan Yang is an assistant professor in the Department of Applied Physics and Applied Mathematics, Columbia University. He received his B.S. in physics from Peking University in 2007 and his Ph.D. in materials science and engineering from Stanford University in 2012. Then he worked as a postdoctoral researcher at MIT for 3 years. His research interests include electrochemical energy storage and conversion and thermal management.

■ ACKNOWLEDGMENTS

Y.Y. acknowledges support from startup funding from Columbia University. This work is partially supported by the NSF MRSEC program through Columbia in the Center for Precision Assembly of Superstratic and Superatomic Solids (DMR-1420634). S.W.L. acknowledges the support by Academic Research Fund Tier 1 from the Ministry of Education, Singapore under ref. no. RG 84/16 and Science and Engineering Research Council Singapore-Korea Joint Research Programme from A*STAR, Singapore under ref. no. 162-82-00009.

■ REFERENCES

(1) Mellit, A.; Massi Pavan, A.; Lughi, V. Short-term forecasting of power production in a large-scale photovoltaic plant. *Sol. Energy* **2014**, *105*, 401−413.

(2) Şimşek, Ş.; Yıldırım, N.; Gülgör, A. Developmental and environmental effects of the Kızıldere geothermal power project, Turkey. *Geothermics* **2005**, *34*, 234−251.

(3) Xue, Y.; Tian, H.; Yan, J.; Zhou, Z.; Wang, J.; Nie, L.; Pan, T.; Zhou, J.; Hua, S.; Wang, Y.; et al. Temporal trends and spatial variation characteristics of primary air pollutants emissions from coal-fired industrial boilers in Beijing, China. *Environ. Pollut.* **2016**, *213*, 717−26.

(4) Hoffert, M. I.; Caldeira, K.; Benford, G.; Criswell, D. R.; Green, C.; Herzog, H.; Jain, A. K.; Kheshgi, H. S.; Lackner, K. S.; Lewis, J. S.; et al. Advanced Technology Paths to Global Climate Stability: Energy for a Greenhouse Planet. *Science* **2002**, *298*, 981−987.

(5) Lawrence Livermore National Laboratory. Esitmated U.S. Energy Use in 2016: 97.3 Quads. https://flowcharts.llnl.gov/content/assets/images/energy/us/Energy_US_2016.png, 2016.

(6) Zebarjadi, M.; Esfarjani, K.; Dresselhaus, M. S.; Ren, Z. F.; Chen, G. Perspectives on thermoelectrics: from fundamentals to device applications. *Energy Environ. Sci.* **2012**, *5*, 5147−5162.

(7) Snyder, G. J.; Toberer, E. S. Complex thermoelectric materials. *Nat. Mater.* **2008**, *7*, 105−114.

(8) Poudel, B.; Hao, Q.; Ma, Y.; Lan, Y.; Minnich, A.; Yu, B.; Yan, X.; Wang, D.; Muto, A.; Vashaee, D.; et al. High-thermoelectric performance of nanostructured bismuth antimony telluride bulk alloys. *Science* **2008**, *320*, 634−638.

(9) deBethune, A. J.; Licht, T. S.; Swendeman, N. The temperature coefficients of electrode potentials - the isothermal and thermal coefficients - the standard ionic entropy of electrochemical transport of the hydrogen ion. *J. Electrochem. Soc.* **1959**, *106*, 616−625.

(10) Salazar, P. F.; Kumar, S.; Cola, B. A. Nitrogen- and Boron-Doped Carbon Nanotube Electrodes in a Thermo-Electrochemical Cell. *J. Electrochem. Soc.* **2012**, *159*, B483−B488.

(11) Salazar, P. F.; Stephens, S. T.; Kazim, A. H.; Pringle, J. M.; Cola, B. A. Enhanced thermo-electrochemical power using carbon nanotube additives in ionic liquid redox electrolytes. *J. Mater. Chem. A* **2014**, *2*, 20676−20682.

(12) Hu, R.; Cola, B. A.; Haram, N.; Barisci, J. N.; Lee, S.; Stoughton, S.; Wallace, G.; Too, C.; Thomas, M.; Gestos, A.; et al. Harvesting Waste Thermal Energy Using a Carbon-Nanotube-Based Thermo-Electrochemical Cell. *Nano Lett.* **2010**, *10*, 838−846.

(13) Gunawan, A.; Lin, C.-H.; Buttry, D. A.; Mujica, V.; Taylor, R. A.; Prasher, R. S.; Phelan, P. E. Liquid Thermoelectrics: Review of Recent And Limited New Data of Thermogalvanic Cell Experiments. *Nanoscale Microscale Thermophys. Eng.* **2013**, *17*, 304−323.

(14) Quickenden, T. I.; Vernon, C. F. Thermogalvanic conversion of heat to electricity. *Sol. Energy* **1986**, *36*, 63−72.

(15) Romano, M. S.; Li, N.; Antiohos, D.; Razal, J. M.; Nattestad, A.; Beirne, S.; Fang, S.; Chen, Y.; Jalili, R.; Wallace, G. G.; et al. Carbon Nanotube - Reduced Graphene Oxide Composites for Thermal Energy Harvesting Applications. *Adv. Mater.* **2013**, *25*, 6602−6606.

(16) Hudak, N. S.; Amatucci, G. G. Energy Harvesting and Storage with Lithium-Ion Thermogalvanic Cells. *J. Electrochem. Soc.* **2011**, *158*, A572−A579.

(17) Chum, H. L.; Osteryoung, R. A. *Review of Thermally Regenerative Electrochemical Systems*; Solar Energy Research Institute: Golden, CO, 1981.

(18) Hammond, R. H.; Risen, W. M. Electrochemical Heat Engine for Direct Solar-energy Conversion. *Sol. Energy* **1979**, *23*, 443−449.

(19) Zhang, F.; Liu, J.; Yang, W.; Logan, B. E. A thermally regenerative ammonia-based battery for efficient harvesting of low-grade thermal energy as electrical power. *Energy Environ. Sci.* **2015**, *8*, 343−349.

(20) Lee, S. W.; Yang, Y.; Lee, H.-W.; Ghasemi, H.; Kraemer, D.; Chen, G.; Cui, Y. An electrochemical system for efficiently harvesting low-grade heat energy. *Nat. Commun.* **2014**, *5*, 3942.

(21) Yang, Y.; Lee, S. W.; Ghasemi, H.; Loomis, J.; Li, X.; Kraemer, D.; Zheng, G.; Cui, Y.; Chen, G. Charging-free electrochemical system for harvesting low-grade thermal energy. *Proc. Natl. Acad. Sci. U. S. A.* **2014**, *111*, 17011−17016.

(22) Hartel, A.; Janssen, M.; Weingarth, D.; Presser, V.; van Roij, R. Heat-to-current conversion of low-grade heat from a thermocapacitive cycle by supercapacitors. *Energy Environ. Sci.* **2015**, *8*, 2396−2401.

(23) Luo, C.; Huang, R.; Kevorkyants, R.; Pavanello, M.; He, H.; Wang, C. Self-Assembled Organic Nanowires for High Power Density Lithium Ion Batteries. *Nano Lett.* **2014**, *14*, 1596−1602.

(24) Tang, Y.; Zhang, Y.; Li, W.; Ma, B.; Chen, X. Rational material design for ultrafast rechargeable lithium-ion batteries. *Chem. Soc. Rev.* **2015**, *44*, 5926−5940.

(25) Case, W. E. *Apparatus for Converting Heat Energy into Electrical Energy*. U.S. Patent 374,173, Dec. 6, 1887.

(26) Quickenden, T. I.; Vernon, C. F. Thermogalvanic conversion of heat to electricity. *Sol. Energy* **1986**, *36*, 63−72.

(27) Zhang, F.; LaBarge, N.; Yang, W.; Liu, J.; Logan, B. E. Enhancing Low-Grade Thermal Energy Recovery in a Thermally Regenerative Ammonia Battery Using Elevated Temperatures. *ChemSusChem* **2015**, *8*, 1043−1048.

(28) Yang, Y.; Loomis, J.; Ghasemi, H.; Lee, S. W.; Wang, Y. J.; Cui, Y.; Chen, G. Membrane-Free Battery for Harvesting Low-Grade Thermal Energy. *Nano Lett.* **2014**, *14*, 6578−6583.

(29) Wessells, C. D.; Huggins, R. A.; Cui, Y. Copper hexacyanoferrate battery electrodes with long cycle life and high power. *Nat. Commun.* **2011**, *2*, 550.

(30) Bratsch, S. G. Standard Electrode Potentials and Temperature Coefficients in Water at 298.15 K. *J. Phys. Chem. Ref. Data* **1989**, *18*, 1−21.

(31) Carlsson, J.; Aqvist, J. Absolute Hydration Entropies of Alkali Metal Ions from Molecular Dynamics Simulations. *J. Phys. Chem. B* **2009**, *113*, 10255−10260.

(32) Florian, J.; Warshel, A. Calculations of hydration entropies of hydrophobic, polar, and ionic solutes in the framework of the Langevin dipoles solvation model. *J. Phys. Chem. B* **1999**, *103*, 10282−10288.

(33) Fultz, B. Vibrational thermodynamics of materials. *Prog. Mater. Sci.* **2010**, *55*, 247−352.

(34) Zhou, F.; Maxisch, T.; Ceder, G. Configurational electronic entropy and the phase diagram of mixed-valence oxides: The case of LixFePO4. *Phys. Rev. Lett.* **2006**, *97*, 155704.

(35) Reynier, Y.; Graetz, J.; Swan-Wood, T.; Rez, P.; Yazami, R.; Fultz, B. Entropy of li intercalation in LixCoO2. *Phys. Rev. B: Condens. Matter Mater. Phys.* **2004**, *70*, 174304.

(36) Viswanathan, V. V.; Choi, D.; Wang, D.; Xu, W.; Towne, S.; Williford, R. E.; Zhang, J.-G.; Liu, J.; Yang, Z. Effect of entropy change of lithium intercalation in cathodes and anodes on Li-ion battery thermal management. *J. Power Sources* **2010**, *195*, 3720−3729.

(37) Zhang, Y.; Cai, W.; Si, F.; Ge, J.; Liang, L.; Liu, C.; Xing, W. A modified Nafion membrane with extremely low methanol permeability via surface coating of sulfonated organic silica. *Chem. Commun.* **2012**, *48*, 2870−2872.

(38) White, N.; Misovich, M.; Yaroshchuk, A.; Bruening, M. L. Coating of Nafion Membranes with Polyelectrolyte Multilayers to Achieve High Monovalent/Divalent Cation Electrodialysis Selectivities. *ACS Appl. Mater. Interfaces* **2015**, *7*, 6620−6628.

(39) Yu, X.; Gross, M. M.; Wang, S.; Manthiram, A. Aqueous Electrochemical Energy Storage with a Mediator-Ion Solid Electrolyte. *Adv. Energy Mater.* **2017**, *7*, 1602454.

(40) Zhai, H.; Xu, P.; Ning, M.; Cheng, Q.; Mandal, J.; Yang, Y. A Flexible Solid Composite Electrolyte with Vertically Aligned and Connected Ion-Conducting Nanoparticles for Lithium Batteries. *Nano Lett.* **2017**, *17*, 3182−3187.

(41) Kang, B.; Ceder, G. Battery materials for ultrafast charging and discharging. *Nature* **2009**, *458*, 190−193.

(42) Long, R.; Li, B.; Liu, Z.; Liu, W. Performance analysis of a thermally regenerative electrochemical cycle for harvesting waste heat. *Energy* **2015**, *87*, 463−469.